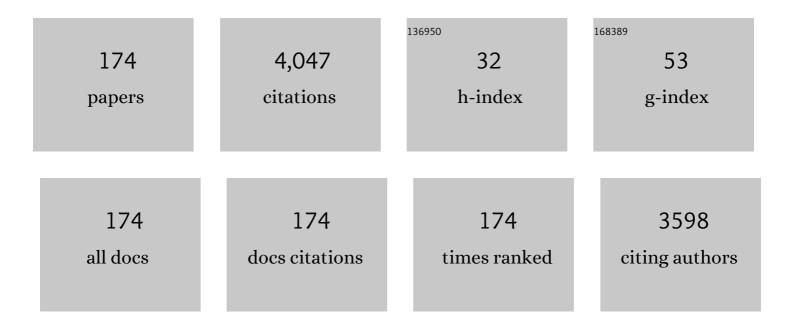
List of Publications by Year in descending order

Source: https://exaly.com/author-pdf/5138944/publications.pdf Version: 2024-02-01



#	Article	IF	CITATIONS
1	Mutational Analysis of Mycobacterial F-ATP Synthase Subunit δ Leads to a Potent δ Enzyme Inhibitor. ACS Chemical Biology, 2022, 17, 529-535.	3.4	6
2	Anti-Mycobacterium abscessus Activity of Tuberculosis F-ATP Synthase Inhibitor GaMF1. Antimicrobial Agents and Chemotherapy, 2022, 66, e0001822.	3.2	4
3	Atomic solution structure of <i>Mycobacterium abscessus</i> <scp>Fâ€ATP</scp> synthase subunit ε and identification of <scp>Ep1<i>Mab</i>F1</scp> as a targeted inhibitor. FEBS Journal, 2022, 289, 6308-6323.	4.7	5
4	Structural and Mechanistic Insights into <i>Mycobacterium abscessus</i> Aspartate Decarboxylase PanD and a Pyrazinoic Acid-Derived Inhibitor. ACS Infectious Diseases, 2022, 8, 1324-1335.	3.8	4
5	A systematic assessment of mycobacterial F ₁ â€ATPase subunit ε's role in latent ATPase hydrolysis. FEBS Journal, 2021, 288, 818-836.	4.7	11
6	Targeting the menaquinol binding loop of mycobacterial cytochrome bd oxidase. Molecular Diversity, 2021, 25, 517-524.	3.9	17
7	Atomic structure of and valine binding to the regulatory ACT domain of the Mycobacterium tuberculosis Rel protein. FEBS Journal, 2021, 288, 2377-2397.	4.7	4
8	Structure of <i>Arabidopsis</i> CESA3 catalytic domain with its substrate UDP-glucose provides insight into the mechanism of cellulose synthesis. Proceedings of the National Academy of Sciences of the United States of America, 2021, 118, .	7.1	22
9	<i>Mycobacterium tuberculosis</i> PanD Structure–Function Analysis and Identification of a Potent Pyrazinoic Acid-Derived Enzyme Inhibitor. ACS Chemical Biology, 2021, 16, 1030-1039.	3.4	9
10	Dual inhibition of the terminal oxidases eradicates antibioticâ€ŧolerant <i>Mycobacterium tuberculosis</i> . EMBO Molecular Medicine, 2021, 13, e13207.	6.9	47
11	Atomic structure of the regulatory TGS domain of Rel protein from Mycobacterium tuberculosis and its interaction with deacylated tRNA. FEBS Letters, 2021, 595, 3006.	2.8	3
12	Targeting Mycobacterial F-ATP Synthase C-Terminal α Subunit Interaction Motif on Rotary Subunit γ. Antibiotics, 2021, 10, 1456.	3.7	8
13	Unique structural and mechanistic properties of mycobacterial F-ATP synthases: Implications for drug design. Progress in Biophysics and Molecular Biology, 2020, 152, 64-73.	2.9	22
14	Overexpression, purification, enzymatic and microscopic characterization of recombinant mycobacterial F-ATP synthase. Biochemical and Biophysical Research Communications, 2020, 522, 374-380.	2.1	8
15	The Unique C-Terminal Extension of Mycobacterial F-ATP Synthase Subunit α Is the Major Contributor to Its Latent ATP Hydrolysis Activity. Antimicrobial Agents and Chemotherapy, 2020, 64, .	3.2	12
16	Features and Functional Importance of Key Residues of the <i>Mycobacterium tuberculosis</i> Cytochrome <i>bd</i> Oxidase. ACS Infectious Diseases, 2020, 6, 1697-1707.	3.8	11
17	3D reconstruction and flexibility of the hybrid engine Acetobacterium woodii F-ATP synthase. Biochemical and Biophysical Research Communications, 2020, 527, 518-524.	2.1	1
18	Residues of helix ɑ2 are critical for catalytic efficiency of mycobacterial alkylhydroperoxide reductase subunit C. FEBS Letters, 2020, 594, 2829-2839.	2.8	0

#	Article	IF	CITATIONS
19	Antituberculosis Activity of the Antimalaria Cytochrome <i>bcc</i> Oxidase Inhibitor SCR0911. ACS Infectious Diseases, 2020, 6, 725-737.	3.8	10
20	Introduction: Novel insights into TB research and drug discovery. Progress in Biophysics and Molecular Biology, 2020, 152, 2-5.	2.9	14
21	Discovery of a Novel Mycobacterial Fâ€ATP Synthase Inhibitor and its Potency in Combination with Diarylquinolines. Angewandte Chemie, 2020, 132, 13397-13406.	2.0	4
22	Pyrazinamide triggers degradation of its target aspartate decarboxylase. Nature Communications, 2020, 11, 1661.	12.8	66
23	Discovery of a Novel Mycobacterial Fâ€ATP Synthase Inhibitor and its Potency in Combination with Diarylquinolines. Angewandte Chemie - International Edition, 2020, 59, 13295-13304.	13.8	28
24	TBAJ-876 Displays Bedaquiline-Like Mycobactericidal Potency without Retaining the Parental Drug's Uncoupler Activity. Antimicrobial Agents and Chemotherapy, 2020, 64, .	3.2	22
25	TBAJ-876 Retains Bedaquiline's Activity against Subunits c and ε of <i>Mycobacterium tuberculosis</i> F-ATP Synthase. Antimicrobial Agents and Chemotherapy, 2019, 63, .	3.2	37
26	Pharmacological and Molecular Mechanisms Behind the Sterilizing Activity of Pyrazinamide. Trends in Pharmacological Sciences, 2019, 40, 930-940.	8.7	35
27	Disrupting coupling within mycobacterial F-ATP synthases subunit ε causes dysregulated energy production and cell wall biosynthesis. Scientific Reports, 2019, 9, 16759.	3.3	29
28	Abundant neuroprotective chaperone Lipocalin-type prostaglandin D synthase (L-PGDS) disassembles the Amyloid-β fibrils. Scientific Reports, 2019, 9, 12579.	3.3	31
29	Structure and subunit arrangement of Mycobacterial F1FO ATP synthase and novel features of the unique mycobacterial subunit l´. Journal of Structural Biology, 2019, 207, 199-208.	2.8	22
30	Effect of the additional cysteine 503 of vancomycin-resistant Enterococcus faecalis (V583) alkylhydroperoxide reductase subunit F (AhpF) and the mechanism of AhpF and subunit C assembling. Free Radical Biology and Medicine, 2019, 138, 10-22.	2.9	1
31	Zika virus nonstructural protein 5 residue R681 is critical for dimer formation and enzymatic activity. FEBS Letters, 2019, 593, 1272-1291.	2.8	6
32	Zika Virus NS5 Forms Supramolecular Nuclear Bodies That Sequester Importin-α and Modulate the Host Immune and Pro-Inflammatory Response in Neuronal Cells. ACS Infectious Diseases, 2019, 5, 932-948.	3.8	34
33	The structural features of AcetobacteriumÂwoodii F―ATP synthase reveal the importance of the unique subunit γâ€koop in Na + translocation and ATP synthesis. FEBS Journal, 2019, 286, 1894-1907.	4.7	4
34	Re-Understanding the Mechanisms of Action of the Anti-Mycobacterial Drug Bedaquiline. Antibiotics, 2019, 8, 261.	3.7	37
35	Structure and flexibility of non-structural proteins 3 and -5 of Dengue- and Zika viruses in solution. Progress in Biophysics and Molecular Biology, 2019, 143, 67-77.	2.9	4
36	Conformational states of Zika virus non-structural protein 3 determined by molecular dynamics simulations with small-angle X-Ray scattering data. Progress in Biophysics and Molecular Biology, 2019, 143, 13-19.	2.9	0

#	Article	IF	CITATIONS
37	Structural model of a2-subunit N-terminus and its binding interface for Arf-GEF CTH2: Implication for regulation of V-ATPase, CTH2 function and rational drug design. Current Topics in Membranes, 2019, 83, 77-106.	0.9	4
38	Active site CP-loop dynamics modulate substrate binding, catalysis, oligomerization, stability, over-oxidation and recycling of 2-Cys Peroxiredoxins. Free Radical Biology and Medicine, 2018, 118, 59-70.	2.9	7
39	Substrateâ€induced structural alterations of Mycobacterial mycothione reductase and critical residues involved. FEBS Letters, 2018, 592, 568-585.	2.8	4
40	The <scp>NMR</scp> solution structure of <i>Mycobacterium tuberculosis</i> Fâ€ <scp>ATP</scp> synthase subunit ε provides new insight into energy coupling inside the rotary engine. FEBS Journal, 2018, 285, 1111-1128.	4.7	37
41	Atomic structure and enzymatic insights into the vancomycin-resistant Enterococcus faecalis (V583) alkylhydroperoxide reductase subunit C. Free Radical Biology and Medicine, 2018, 115, 252-265.	2.9	9
42	Crystallographic and enzymatic insights into the mechanisms of Mg-ADP inhibition in the A1 complex of the A1AO ATP synthase. Journal of Structural Biology, 2018, 201, 26-35.	2.8	4
43	Targeting the Mycobacterium ulcerans cytochrome bc1:aa3 for the treatment of Buruli ulcer. Nature Communications, 2018, 9, 5370.	12.8	64
44	Molecular mechanism of the Escherichia coli AhpC in the function of a chaperone under heat-shock conditions. Scientific Reports, 2018, 8, 14151.	3.3	11
45	Structure and function of Mycobacterium-specific components of F-ATP synthase subunits α and Îμ. Journal of Structural Biology, 2018, 204, 420-434.	2.8	9
46	Partial Intrinsic Disorder Governs the Dengue Capsid Protein Conformational Ensemble. ACS Chemical Biology, 2018, 13, 1621-1630.	3.4	18
47	Self-association and conformational variation of NS5A domain 1 of hepatitis C virus. Journal of General Virology, 2018, 99, 194-208.	2.9	2
48	Analyzing conformational changes in single FRET-labeled A1 parts of archaeal A1AO-ATP synthase. , 2018, , .		0
49	Structural features of Zika virus non-structural proteins 3 and -5 and its individual domains in solution as well as insights into NS3 inhibition. Antiviral Research, 2017, 141, 73-90.	4.1	24
50	Conformational dynamics of the rotary subunit F in the A ₃ B ₃ <scp>DF</scp> complex of <i>Methanosarcina mazei</i> Gö1 Aâ€ <scp>ATP</scp> synthase monitored by singleâ€molecule <scp>FRET</scp> . FEBS Letters, 2017, 591, 854-862.	2.8	8
51	Essential role of the flexible linker on the conformational equilibrium of bacterial peroxiredoxin reductase for effective regeneration of peroxiredoxin. Journal of Biological Chemistry, 2017, 292, 6667-6679.	3.4	5
52	The uniqueness of subunit α of mycobacterial F-ATP synthases: An evolutionary variant for niche adaptation. Journal of Biological Chemistry, 2017, 292, 11262-11279.	3.4	33
53	Structural and mechanistic insights into Mycothiol Disulphide Reductase and the Mycoredoxin-1-alkylhydroperoxide reductase E assembly of Mycobacterium tuberculosis. Biochimica Et Biophysica Acta - General Subjects, 2017, 1861, 2354-2366.	2.4	9
54	Structural features of NS3 of <i>Dengue virus</i> serotypes 2 and 4 in solution and insight into RNA binding and the inhibitory role of quercetin. Acta Crystallographica Section D: Structural Biology, 2017, 73, 402-419.	2.3	12

#	Article	IF	CITATIONS
55	Pyrazinoic Acid Inhibits Mycobacterial Coenzyme A Biosynthesis by Binding to Aspartate Decarboxylase PanD. ACS Infectious Diseases, 2017, 3, 807-819.	3.8	52
56	Novel insights into the vancomycin-resistant Enterococcus faecalis (V583) alkylhydroperoxide reductase subunit F. Biochimica Et Biophysica Acta - General Subjects, 2017, 1861, 3201-3214.	2.4	2
57	Crystallographic and solution structure of the Nâ€ŧerminal domain of the Rel protein from <i>Mycobacterium tuberculosis</i> . FEBS Letters, 2017, 591, 2323-2337.	2.8	27
58	AhpC of the mycobacterial antioxidant defense system and its interaction with its reducing partner Thioredoxin-C. Scientific Reports, 2017, 7, 5159.	3.3	20
59	Exploiting the synthetic lethality between terminal respiratory oxidases to kill <i>Mycobacterium tuberculosis</i> and clear host infection. Proceedings of the National Academy of Sciences of the United States of America, 2017, 114, 7426-7431.	7.1	141
60	Temperature effects on disk-like gold-nickel-platinum nanoswimmer's propulsion fuelled by hydrogen peroxide. Sensors and Actuators B: Chemical, 2017, 239, 586-596.	7.8	12
61	Deletion of a unique loop in the mycobacterial Fâ€ <scp>ATP</scp> synthase γ subunit sheds light on its inhibitory role in <scp>ATP</scp> hydrolysisâ€driven H ⁺ pumping. FEBS Journal, 2016, 283, 1947-1961.	4.7	43
62	Transition steps in peroxide reduction and a molecular switch for peroxide robustness of prokaryotic peroxiredoxins. Scientific Reports, 2016, 6, 37610.	3.3	20
63	Power Stroke Angular Velocity Profiles of Archaeal A-ATP Synthase Versus Thermophilic and Mesophilic F-ATP Synthase Molecular Motors. Journal of Biological Chemistry, 2016, 291, 25351-25363.	3.4	25
64	Redox chemistry of Mycobacterium tuberculosis alkylhydroperoxide reductase E (AhpE): Structural and mechanistic insight into a mycoredoxin-1 independent reductive pathway of AhpE via mycothiol. Free Radical Biology and Medicine, 2016, 97, 588-601.	2.9	19
65	Bedaquiline Targets the ε Subunit of Mycobacterial F-ATP Synthase. Antimicrobial Agents and Chemotherapy, 2016, 60, 6977-6979.	3.2	58
66	Hydrogen-peroxide-fuelled platinum–nickel–SU-8 microrocket with steerable propulsion using an eccentric nanoengine. RSC Advances, 2016, 6, 102513-102518.	3.6	8
67	Identification of the critical linker residues conferring differences in the compactness of NS5 from <i>Dengue virus</i> serotype 4 and NS5 from <i>Dengue virus</i> serotypes 1–3. Acta Crystallographica Section D: Structural Biology, 2016, 72, 795-807.	2.3	14
68	The stimulating role of subunit F in ATPase activity inside the A1-complex of the Methanosarcina mazei Gö1 A1AO ATP synthase. Biochimica Et Biophysica Acta - Bioenergetics, 2016, 1857, 177-187.	1.0	10
69	Eukaryotic V-ATPase and Its Super-complexes: From Structure and Function to Disease and Drug Targeting. , 2016, , 301-335.		3
70	Disk-like nanojets with steerable trajectory using platinum nozzle nanoengines. RSC Advances, 2016, 6, 3399-3405.	3.6	12
71	Low resolution solution structure of an enzymatic active AhpC 10 :AhpF 2 ensemble of the Escherichia coli Alkyl hydroperoxide Reductase. Journal of Structural Biology, 2016, 193, 13-22.	2.8	10
72	<scp>NMR</scp> studies reveal a novel grab and release mechanism for efficient catalysis of the bacterial 2â€Cys peroxiredoxin machinery. FEBS Journal, 2015, 282, 4620-4638.	4.7	9

#	Article	IF	CITATIONS
73	Crystal Structure of Subunits D and F in Complex Gives Insight into Energy Transmission of the Eukaryotic V-ATPase from Saccharomyces cerevisiae. Journal of Biological Chemistry, 2015, 290, 3183-3196.	3.4	38
74	The Molecular Motor F-ATP Synthase Is Targeted by the Tumoricidal Protein HAMLET. Journal of Molecular Biology, 2015, 427, 1866-1874.	4.2	29
75	The C-terminal 50 Amino Acid Residues of Dengue NS3 Protein Are Important for NS3-NS5 Interaction and Viral Replication. Journal of Biological Chemistry, 2015, 290, 2379-2394.	3.4	105
76	Crystallographic and solution studies of NAD+- and NADH-bound alkylhydroperoxide reductase subunit F (AhpF) from Escherichia coli provide insight into sequential enzymatic steps. Biochimica Et Biophysica Acta - Bioenergetics, 2015, 1847, 1139-1152.	1.0	12
77	Structural insight and flexible features of NS5 proteins from all four serotypes of <i>Dengue virus</i> in solution. Acta Crystallographica Section D: Biological Crystallography, 2015, 71, 2309-2327.	2.5	34
78	Protein–protein interactions within the ensemble, eukaryotic V-ATPase, and its concerted interactions with cellular machineries. Progress in Biophysics and Molecular Biology, 2015, 119, 84-93.	2.9	2
79	Crystallographic structure of the turbine <i>C</i> -ring from spinach chloroplast F-ATP synthase. Bioscience Reports, 2014, 34, .	2.4	9
80	Transamidase subunit GAA1/GPAA1 is a M28 family metallo-peptide-synthetase that catalyzes the peptide bond formation between the substrate protein's omega-site and the GPI lipid anchor's phosphoethanolamine. Cell Cycle, 2014, 13, 1912-1917.	2.6	41
81	Structure, mechanism and ensemble formation of the alkylhydroperoxide reductase subunits AhpC and AhpF from <i>Escherichia coli</i> . Acta Crystallographica Section D: Biological Crystallography, 2014, 70, 2848-2862.	2.5	47
82	ATP synthases from archaea: The beauty of a molecular motor. Biochimica Et Biophysica Acta - Bioenergetics, 2014, 1837, 940-952.	1.0	98
83	Eukaryotic V-ATPase: Novel structural findings and functional insights. Biochimica Et Biophysica Acta - Bioenergetics, 2014, 1837, 857-879.	1.0	150
84	Key roles of the Escherichia coli AhpC C-terminus in assembly and catalysis of alkylhydroperoxide reductase, an enzyme essential for the alleviation of oxidative stress. Biochimica Et Biophysica Acta - Bioenergetics, 2014, 1837, 1932-1943.	1.0	21
85	Solution structure of subunit γ (γ1-204) of the Mycobacterium tuberculosis F-ATP synthase and the unique loop of γ165-178, representing a novel TB drug target. Journal of Bioenergetics and Biomembranes, 2013, 45, 121-129.	2.3	16
86	The DNA uptake ATPase PilF of Thermus thermophilus: a reexamination of the zinc content. Extremophiles, 2013, 17, 697-698.	2.3	6
87	Conformational Properties of Secondary Amino Acids: Replacement of Pipecolic Acid by <i>N</i> â€Methylâ€ <scp>L</scp> â€alanine in Efrapeptin C. Chemistry and Biodiversity, 2013, 10, 942-951.	2.1	9
88	The N Termini of a-Subunit Isoforms Are Involved in Signaling between Vacuolar H+-ATPase (V-ATPase) and Cytohesin-2*. Journal of Biological Chemistry, 2013, 288, 5896-5913.	3.4	42
89	Low-resolution structure of the soluble domain GPAA1 (yGPAA170–247) of the glycosylphosphatidylinositol transamidase subunit GPAA1 from Saccharomyces cerevisiae. Bioscience Reports, 2013, 33, e00033.	2.4	6
90	Crystal and NMR Structures Give Insights into the Role and Dynamics of Subunit F of the Eukaryotic V-ATPase from Saccharomyces cerevisiae. Journal of Biological Chemistry, 2013, 288, 11930-11939.	3.4	10

#	Article	IF	CITATIONS
91	Variations of Subunit ε of the Mycobacterium tuberculosis F ₁ F ₀ ATP Synthase and a Novel Model for Mechanism of Action of the Tuberculosis Drug TMC207. Antimicrobial Agents and Chemotherapy, 2013, 57, 168-176.	3.2	64
92	Novel role of cytohesinâ€2 in regulation of macropinocytosis pathway and cell proliferation. FASEB Journal, 2013, 27, 591.8.	0.5	0
93	Crystallization and preliminary X-ray crystallographic analysis of subunit F (F1–94), an essential coupling subunit of the eukaryotic V1VO-ATPase fromSaccharomyces cerevisiae. Acta Crystallographica Section F: Structural Biology Communications, 2012, 68, 1055-1059.	0.7	3
94	Structural architecture and interplay of the nucleotide- and erythrocyte binding domain of the reticulocyte binding protein Py235 from Plasmodium yoelii. International Journal for Parasitology, 2012, 42, 1083-1089.	3.1	4
95	Relevance of the conserved histidine and asparagine residues in the phosphate-binding loop of the nucleotide binding subunit B of A1AO ATP synthases. Journal of Structural Biology, 2012, 180, 509-518.	2.8	3
96	The Structure of Subunit E of the Pyrococcus horikoshii OT3 A-ATP Synthase Gives Insight into the Elasticity of the Peripheral Stalk. Journal of Molecular Biology, 2012, 420, 155-163.	4.2	14
97	Low Resolution Solution Structure of HAMLET and the Importance of Its Alpha-Domains in Tumoricidal Activity. PLoS ONE, 2012, 7, e53051.	2.5	25
98	Subunit F modulates ATP binding and migration in the nucleotide-binding subunit B of the A1AO ATP synthase of Methanosarcina mazei GA¶1. Journal of Bioenergetics and Biomembranes, 2012, 44, 213-224.	2.3	3
99	Solution structure of subunit a, a 104-363, of the Saccharomyces cerevisiae V-ATPase and the importance of its C-terminus in structure formation. Journal of Bioenergetics and Biomembranes, 2012, 44, 341-350.	2.3	12
100	Solution structure of subunit F (Vma7p) of the eukaryotic V1VO ATPase from Saccharomyces cerevisiae derived from SAXS and NMR spectroscopy. Biochimica Et Biophysica Acta - Biomembranes, 2011, 1808, 360-368.	2.6	9
101	Binding of subunit E into the A–B interface of the A1AO ATP synthase. Biochimica Et Biophysica Acta - Biomembranes, 2011, 1808, 2111-2118.	2.6	4
102	Structural insight into the glycosylphosphatidylinositol transamidase subunits PIG-K and PIG-S from yeast. Journal of Structural Biology, 2011, 173, 271-281.	2.8	12
103	The Transition-Like State and Pi Entrance into the Catalytic A Subunit of the Biological Engine A-ATP Synthase. Journal of Molecular Biology, 2011, 408, 736-754.	4.2	9
104	Conserved Glycine Residues in the P-Loop of ATP Synthases Form a Doorframe for Nucleotide Entrance. Journal of Molecular Biology, 2011, 413, 657-666.	4.2	7
105	NMR solution structure of NBD94483-502 of the nucleotide-binding domain of the Plasmodium yoelii reticulocyte-binding protein Py235. FEMS Microbiology Letters, 2011, 318, 152-158.	1.8	3
106	NMR solution structure of subunit E (fragment E1–69) of the Saccharomyces cerevisiae V1VO ATPase. Journal of Bioenergetics and Biomembranes, 2011, 43, 187-193.	2.3	7
107	Structural elements of the C-terminal domain of subunit E (E133-222) from the Saccharomyces cerevisiae V1VO ATPase determined by solution NMR spectroscopy. Journal of Bioenergetics and Biomembranes, 2011, 43, 447-455.	2.3	9
108	Identification and characterization of a unique, zinc-containing transport ATPase essential for natural transformation in Thermus thermophilus HB27. Extremophiles, 2011, 15, 191-202.	2.3	26

#	Article	IF	CITATIONS
109	Purification and crystallization of yeast glycosylphosphatidylinositol transamidase subunit PIG-S (PIG-S71–467). Acta Crystallographica Section F: Structural Biology Communications, 2011, 67, 896-899.	0.7	3
110	Engineered tryptophan in the adenine-binding pocket of catalytic subunit A of A-ATP synthase demonstrates the importance of aromatic residues in adenine binding, forming a tool for steady-state and time-resolved fluorescence spectroscopy. Acta Crystallographica Section F: Structural Biology Communications, 2011, 67, 1485-1491.	0.7	0
111	Structural Characterization of the Erythrocyte Binding Domain of the Reticulocyte Binding Protein Homologue Family of Plasmodium yoelii. Infection and Immunity, 2011, 79, 2880-2888.	2.2	11
112	Specific motifs of the V-ATPase a2-subunit isoform interact with catalytic and regulatory domains of ARNO. Biochimica Et Biophysica Acta - Bioenergetics, 2010, 1797, 1398-1409.	1.0	33
113	The effect of NBD-Cl in nucleotide-binding of the major subunit $\hat{I}\pm$ and B of the motor proteins F1FO ATP synthase and A1AO ATP synthase. Journal of Bioenergetics and Biomembranes, 2010, 42, 1-10.	2.3	2
114	Crystal and solution structure of the C-terminal part of the Methanocaldococcus jannaschii A1AO ATP synthase subunit E revealed by X-ray diffraction and small-angle X-ray scattering. Journal of Bioenergetics and Biomembranes, 2010, 42, 311-320.	2.3	5
115	Crystallographic insight into the catalytic mechanism of subunit A of the A-ATP synthase and the P-loop switch in evolution. Biochimica Et Biophysica Acta - Bioenergetics, 2010, 1797, 32-33.	1.0	Ο
116	Disulfide linkage in the coiled oil domain of subunit H of A ₁ A _O ATP synthase from <i>Methanocaldococcus jannaschii</i> and the NMR structure of the Câ€ŧerminal segment H _{85–104} . FEBS Letters, 2010, 584, 713-718.	2.8	2
117	Purification and crystallization of the entire recombinant subunit E of the energy producer A1AoATP synthase. Acta Crystallographica Section F: Structural Biology Communications, 2010, 66, 324-326.	0.7	4
118	Crystallographic studies of the coupling segment NBD94674–781of the nucleotide-binding domain of thePlasmodium yoeliireticulocyte-binding protein Py235. Acta Crystallographica Section F: Structural Biology Communications, 2010, 66, 1631-1634.	0.7	0
119	Nâ€ŧerminal domain of the Vâ€ATPase a2â€subunit displays integral membrane protein properties. Protein Science, 2010, 19, 1850-1862.	7.6	10
120	Structural Determination of Functional Units of the Nucleotide Binding Domain (NBD94) of the Reticulocyte Binding Protein Py235 of Plasmodium yoelii. PLoS ONE, 2010, 5, e9146.	2.5	9
121	Crosstalk along the Stalk: Dynamics of the Interaction of Subunits B and F in the A ₁ A _O ATP Synthase of <i>Methanosarcina mazei</i> Gö1. Biochemistry, 2010, 49, 4181-4190.	2.5	7
122	Nucleotide Binding States of Subunit A of the A-ATP Synthase and the Implication of P-Loop Switch in Evolution. Journal of Molecular Biology, 2010, 396, 301-320.	4.2	30
123	The Critical Roles of Residues P235 and F236 of Subunit A of the Motor Protein A-ATP Synthase in P-Loop Formation and Nucleotide Binding. Journal of Molecular Biology, 2010, 401, 892-905.	4.2	4
124	The NMR solution structure of subunit G (G61–101) of the eukaryotic V1VO ATPase from Saccharomyces cerevisiae. Biochimica Et Biophysica Acta - Biomembranes, 2010, 1798, 1961-1968.	2.6	9
125	Solution Structure, Determined by Nuclear Magnetic Resonance, of the b30-82 Domain of Subunit b of Escherichia coli F 1 F o ATP Synthase. Journal of Bacteriology, 2009, 191, 7538-7544.	2.2	16
126	Assembly of subunit d (Vma6p) and G (Vma10p) and the NMR solution structure of subunit G (G1–59) of the Saccharomyces cerevisiae V1VO ATPase. Biochimica Et Biophysica Acta - Bioenergetics, 2009, 1787, 242-251.	1.0	14

#	Article	IF	CITATIONS
127	Association of the eukaryotic V ₁ V _O ATPase subunits <i>a</i> with <i>d</i> and <i>d</i> with A. FEBS Letters, 2009, 583, 1090-1095.	2.8	7
128	NMR solution structure of the N-terminal domain of subunit E (E1–52) of A1AO ATP synthase from Methanocaldococcus jannaschii. Journal of Bioenergetics and Biomembranes, 2009, 41, 343-348.	2.3	5
129	Spectroscopic and crystallographic studies of the mutant R416W give insight into the nucleotide binding traits of subunit B of the A ₁ A _o ATP synthase. Proteins: Structure, Function and Bioinformatics, 2009, 75, 807-819.	2.6	22
130	A second transient position of ATP on its trail to the nucleotide-binding site of subunit B of the motor protein A1AO ATP synthase. Journal of Structural Biology, 2009, 166, 38-45.	2.8	9
131	Domain Features of the Peripheral Stalk Subunit H of the Methanogenic A1AO ATP Synthase and the NMR Solution Structure of H1-47. Biophysical Journal, 2009, 97, 286-294.	0.5	6
132	Low resolution structure of subunit b (b 22–156) of Escherichia coli F1FO ATP synthase in solution and the bâ~δassembly. Journal of Bioenergetics and Biomembranes, 2008, 40, 245-55.	2.3	9
133	Structure of the nucleotide-binding subunit B of the energy producer A ₁ A ₀ ATP synthase in complex with adenosine diphosphate. Acta Crystallographica Section D: Biological Crystallography, 2008, 64, 1110-1115.	2.5	10
134	New insights into structureâ€function relationships between archeal ATP synthase (A ₁ A ₀) and vacuolar type ATPase (V ₁ V ₀). BioEssays, 2008, 30, 1096-1109.	2.5	76
135	Identification of critical residues of subunit H in its interaction with subunit E of the Aâ€ATP synthase from <i>Methanocaldococcus jannaschii</i> . FEBS Journal, 2008, 275, 1803-1812.	4.7	10
136	Spectroscopical identification of residues of subunit G of the yeast V-ATPase in its connection with subunit E. Molecular Membrane Biology, 2008, 25, 400-410.	2.0	10
137	Crystal Structure of the NS3 Protease-Helicase from Dengue Virus. Journal of Virology, 2008, 82, 173-183.	3.4	241
138	ATP/ADP Binding to a Novel Nucleotide Binding Domain of the Reticulocyte-binding Protein Py235 of Plasmodium yoelii. Journal of Biological Chemistry, 2008, 283, 36386-36396.	3.4	12
139	Cloning, purification, and nucleotide-binding traits of the catalytic subunit A of the V1VO ATPase from Aedes albopictus. Protein Expression and Purification, 2007, 53, 378-383.	1.3	19
140	NMR Solution Structure of Subunit F of the Methanogenic A1AO Adenosine Triphosphate Synthase and Its Interaction with the Nucleotide-Binding Subunit B,. Biochemistry, 2007, 46, 11684-11694.	2.5	26
141	Small-Angle X-ray Scattering Reveals the Solution Structure of the Peripheral Stalk Subunit H of the A1AO ATP Synthase from Methanocaldococcus jannaschii and Its Binding to the Catalytic A Subunit. Biochemistry, 2007, 46, 2070-2078.	2.5	21
142	The boxing glove shape of subunit d of the yeast V-ATPase in solution and the importance of disulfide formation for folding of this protein. Journal of Bioenergetics and Biomembranes, 2007, 39, 275-289.	2.3	24
143	1H, 13C, and 15N resonance assignments of subunit F of the A1AO ATP synthase from Methanosarcina mazei Gö1. Biomolecular NMR Assignments, 2007, 1, 23-25.	0.8	3
144	A WNK kinase binds and phosphorylates V-ATPase subunit C. FEBS Letters, 2006, 580, 932-939.	2.8	114

#	Article	IF	CITATIONS
145	Crystal Structure of the Archaeal A1AO ATP Synthase Subunit B from Methanosarcina mazei Gö1: Implications of Nucleotide-binding Differences in the Major A1AO Subunits A and B. Journal of Molecular Biology, 2006, 358, 725-740.	4.2	60
146	Structural and functional analysis of the coupling subunit F in solution and topological arrangement of the stalk domains of the methanogenic A1AO ATP synthase. Journal of Bioenergetics and Biomembranes, 2006, 38, 83-92.	2.3	33
147	Evidence for major structural changes in subunit C of the vacuolar ATPase due to nucleotide binding. FEBS Letters, 2005, 579, 1961-1967.	2.8	51
148	Interaction between subunit C (Vma5p) of the yeast vacuolar ATPase and the stalk of the C-depleted V1 ATPase from Manduca sexta midgut. Biochimica Et Biophysica Acta - Bioenergetics, 2005, 1708, 196-200.	1.0	8
149	Structural Characterization of an ATPase Active F1-/V1 -ATPase (α3β3EG) Hybrid Complex. Journal of Biological Chemistry, 2004, 279, 47866-47870.	3.4	5
150	Three-dimensional Organization of the Archaeal A1-ATPase from Methanosarcina mazei Gö1. Journal of Biological Chemistry, 2004, 279, 22759-22764.	3.4	33
151	Structure and Subunit Arrangement of the A-type ATP Synthase Complex from the Archaeon Methanococcus jannaschii Visualized by Electron Microscopy. Journal of Biological Chemistry, 2004, 279, 38644-38648.	3.4	59
152	Ligand-Dependent Structural Changes in the V1ATPase from Manduca sexta. Journal of Bioenergetics and Biomembranes, 2004, 36, 249-256.	2.3	12
153	Structural analysis of the stalk subunit Vma5p of the yeast Vâ€ATPase in solution. FEBS Letters, 2004, 570, 119-125.	2.8	44
154	Introduction: A close look at the vacuolar ATPase. Journal of Bioenergetics and Biomembranes, 2003, 35, 277-280.	2.3	6
155	Defined subcomplexes of the A ₁ ATPase from the archaeon <i>Methanosarcina mazei</i> Gö1: biochemical properties and redox regulation. FEBS Letters, 2003, 544, 206-209.	2.8	17
156	Dimer formation of subunit G of the yeast V-ATPase. FEBS Letters, 2003, 546, 395-400.	2.8	17
157	Resolution of the V1 ATPase from Manduca sexta into Subcomplexes and Visualization of an ATPase-active A3B3EG Complex by Electron Microscopy. Journal of Biological Chemistry, 2003, 278, 270-275.	3.4	29
158	Cross-talk in the A1-ATPase from Methanosarcina mazei Gö1 Due to Nucleotide Binding. Journal of Biological Chemistry, 2002, 277, 17327-17333.	3.4	32
159	Expression, purification, and characterization of subunit E, an essential subunit of the vacuolar ATPase. Biochemical and Biophysical Research Communications, 2002, 298, 383-391.	2.1	69
160	8-N3-3′-Biotinyl-ATP, a Novel Monofunctional Reagent: Differences in the F1- and V1-ATPases by Means of the ATP Analogue. Biochemical and Biophysical Research Communications, 2001, 286, 1218-1227.	2.1	17
161	The Structure of the V1-ATPase Determined by Three-Dimensional Electron Microscopy of Single Particles. Journal of Structural Biology, 2001, 135, 26-37.	2.8	102
162	Structural Insights into the A1 ATPase from the Archaeon, Methanosarcina mazei Gö1. Biochemistry, 2001, 40, 1890-1896.	2.5	42

#	Article	IF	CITATIONS
163	Structural and functional features of the Escherichia coli F1-ATPase. , 2000, 32, 341-346.		16
164	Three-Dimensional Structure and Subunit Topology of the V ₁ ATPase from <i>Manduca sexta</i> Midgut. Biochemistry, 2000, 39, 8609-8616.	2.5	71
165	Solution Structure and Conformational Changes of the Streptomyces Chitin-Binding Protein (CHB1). Biochemistry, 2000, 39, 10677-10683.	2.5	31
166	The plasma membrane H+-V-ATPase from tobacco hornworm midgut. Journal of Bioenergetics and Biomembranes, 1999, 31, 67-74.	2.3	65
167	Molecular architecture of <i>Manduca sexta</i> midgut V ₁ ATPase visualized by electron microscopy. FEBS Letters, 1999, 453, 383-386.	2.8	27
168	Trapping of conformations of theEscherichia coliF1ATPase by disulfide bond formation. FEBS Letters, 1998, 426, 37-40.	2.8	5
169	Quaternary Structure of V1and F1ATPase: Significance of Structural Homologies and Diversitiesâ€. Biochemistry, 1998, 37, 17659-17663.	2.5	56
170	An improved purification of ECF1and ECF1F0by using a cytochromebo-deficient strain ofEscherichia colifacilitates crystallization of these complexes. FEBS Letters, 1997, 410, 165-168.	2.8	11
171	Differentiation of Catalytic Sites onEscherichia coliF1ATPase by Laser Photoactivated Labeling with [3H]-2-Azido-ATP Using the Mutant βGlu381Cys:εSer108Cys To Identify Different β Subunits by Their Interactions with γ and ε Subunitsâ€. Biochemistry, 1996, 35, 3875-3879.	2.5	30
172	Structural changes in the Î ³ and ε subunits of theEscherichia coli F1F0-type ATPase during energy coupling. Journal of Bioenergetics and Biomembranes, 1996, 28, 397-401.	2.3	64
173	The Trapping of Different Conformations of the Escherichia coli F1 ATPase by Disulfide Bond Formation. Journal of Biological Chemistry, 1996, 271, 32623-32628.	3.4	29
174	ATP synthesis and hydrolysis of the ATP-synthase from Micrococcus luteus regulated by an inhibitor subunit and membrane energization. Biochimica Et Biophysica Acta - Bioenergetics, 1994, 1186, 43-51.	1.0	11